

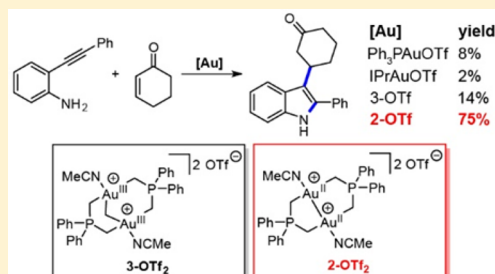
Lewis Acid Catalysis with Cationic Dinuclear Gold(II,II) and Gold(III,III) Phosphorus Ylide Complexes

Benjamin R. Reiner, Mark W. Bezpalko, Bruce M. Foxman, and Casey R. Wade*

Department of Chemistry, Brandeis University, 415 South Street MS 015, Waltham, Massachusetts 02453, United States

S Supporting Information

ABSTRACT: The dinuclear gold(II,II) and gold(III,III) complexes $[\text{Au}_2(\mu\text{-PY})_2(\text{MeCN})_2]\text{OTf}_2$ (**2-OTf₂**) and $[\text{Au}_2(\mu\text{-PY})_2(\mu\text{-CH}_2)(\text{MeCN})_2]\text{OTf}_2$ (**3-OTf₂**) (PY = $[(\text{CH}_2)_2\text{PPh}_2]^-$) have been synthesized and evaluated as Lewis acid catalysts for Mukaiyama addition and alkyne hydroamination reactions. **2-OTf₂** and **3-OTf₂** provide similar or improved catalytic activity for these reactions compared to the commonly used gold(I) Lewis acids Ph_3PAuOTf and IPrAuOTf . The versatile Lewis acidity of **2-OTf₂** was further demonstrated by its superior performance in a cascade reaction involving intramolecular hydroamination followed by intermolecular conjugate addition to generate a 2,3-substituted indole.



INTRODUCTION

Over the past decade, the use of homogeneous gold catalysts for C–C and C–X bond-forming reactions has increased remarkably.^{1–5} Interest in gold-based catalysis stems from its tolerance to oxygen and water, low toxicity, and low proclivity for β -hydride elimination. Moreover, much of the catalytic efficacy of gold is grounded in its soft Lewis acidity, which allows for the activation of unsaturated organic substrates. Complexes containing gold(I) and gold(III) centers have been shown to activate alkenes and alkynes for nucleophilic addition.^{6–8} However, divergent reactivity between gold(I) and gold(III) has been observed in some cases and attributed to differences in hard/soft Lewis acidity.^{9–11} For example, Gevorgyan et al. have reported that Et_3PAuCl and AuCl_3 both catalyze the cyclization of haloallenyl ketones, but generate different isomers of the halofuran products.⁹ More recently, Toste et al. demonstrated that the gold(III) complex $[\text{IPrAu}(\text{biphenyl})]\text{OTf}$ (IPr = *N,N'*-(2,6-diisopropylphenyl)-imidazol-2-ylidene) activates α,β -unsaturated carbonyl compounds for conjugate addition.¹² However, the gold(I) analogue IPrAuOTf exhibited no catalytic activity for the reaction, affirming the contrast in hard/soft Lewis acidity between gold(I) and gold(III) centers.

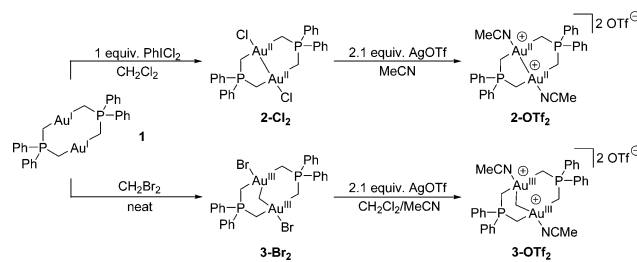
While the catalytic properties of gold(I) and gold(III) have been well-established, those of gold(II) have been relatively unexplored.¹³ Owing to a d^9 electron configuration, gold(II) complexes are typically isolated as multinuclear frameworks containing covalent Au–Au bonds. Several dinucleating ligand platforms have been used to support gold(II) complexes.^{14–16} Among these, phosphorus ylide (PY) ligands have been shown to support rich redox chemistry. Dinuclear gold PY complexes with the metals in the (I,I), (II,II), (I,III), and (III,III) oxidation states have been structurally characterized.^{17–22} The strong σ -donating character of the bridging PY ligands confers excellent stability across the range of oxidation states. This is notable

considering that organogold(III) complexes are often unstable toward reductive elimination.^{23–25} Consequently, we envisaged the dinuclear gold PY framework as a platform for exploring the catalytic activity of well-defined gold(II) and gold(III) centers. While several examples of cationic gold(II,II) and gold(III,III) PY complexes have been reported, few contain combinations of weakly coordinating anions and labile ancillary ligands expected to result in active Lewis acid catalysts.^{26,27} Herein we report the synthesis, characterization, and Lewis acid catalytic activity of dicationic gold(II,II) and gold(III,III) PY complexes containing weakly coordinating OTf^- counteranions and MeCN ancillary ligands.

RESULTS AND DISCUSSION

The dinuclear gold PY complexes **1** and **3-Br₂** were synthesized according to literature procedures.^{18,19,21} Reaction of **1** with PhICl_2 afforded the gold(II,II) complex **2-Cl₂** (Scheme 1). The dicationic complex **2-OTf₂** was isolated as a bright yellow solid after treatment of **2-Cl₂** with AgOTf in acetonitrile solution. Notably, the use of weakly coordinating solvents such as CH_2Cl_2 or THF for this reaction resulted in a mixture of

Scheme 1. Synthesis of 2-OTf₂ and 3-OTf₂



Received: May 18, 2016

decomposition products, suggesting that the dication is stabilized by coordination of MeCN. The $^{31}\text{P}\{^1\text{H}\}$ NMR spectrum of **2-OTf**₂ in CD_2Cl_2 displays a single resonance at 34.5 ppm, shifted slightly upfield from that of **2-Cl**₂ (36.0 ppm). The ^1H NMR spectrum features aromatic resonances consistent with equivalent Ph groups and a doublet at 1.95 ppm assigned to the CH_2 groups of the PY ligand. The presence of a singlet resonance at 2.2 ppm is consistent with two molecules of coordinated MeCN. **2-OTf**₂ is stable to air and moisture but exhibits moderate light sensitivity.

Treatment of **3-Br**₂ with AgOTf in $\text{CH}_2\text{Cl}_2/\text{MeCN}$ solution generated the dicationic complex **3-OTf**₂ as a colorless solid. The complex is stable to air, moisture, and light in both solution and the solid state. The $^{31}\text{P}\{^1\text{H}\}$ NMR spectrum of **3-OTf**₂ in CD_3CN displays a single resonance at 35.1 ppm, shifted slightly upfield from that of **3-Br**₂ (37.5 ppm). The ^1H NMR spectrum shows several diagnostic features that indicate the complex retains a rigid, boat-like conformation in solution.²¹ These features include two sets of aromatic resonances consistent with inequivalent Ph groups. Two virtual triplets, centered at 1.88 and 2.46 ppm, suggest a diastereotopic relationship between the methylene protons of the PY ligand. Singlet resonances at 2.68 and 1.97 ppm are assigned to the $\mu\text{-CH}_2$ ligand and two molecules of coordinated MeCN, respectively.

The solid-state structures of **2-OTf**₂ and **3-OTf**₂ were determined by single-crystal X-ray diffraction. X-ray quality crystals of both complexes were obtained by vapor diffusion of Et_2O into MeCN solutions. **2-OTf**₂ crystallizes in the space group $P\bar{1}$ with one-half molecule of $[\mathbf{2}]^{2+}$, one OTf^- ion, and one interstitial MeCN molecule in the asymmetric unit. The structure of **2-OTf**₂ shows that the eight-membered metallacycle adopts a chair conformation with both gold(II) centers in square planar geometries (Figure 1a). The observed equivalence of the Ph groups by ^1H NMR spectroscopy at room temperature suggests rapid ring flipping of the metallacycle in solution. The $\text{Au}-\text{C}_{\text{PY}}$ distances (2.106(2) and 2.111(2) Å) are comparable to those found in related Au(II,II) complexes.²⁸ Notably, the $\text{Au}-\text{Au}$ intermetallic distance of 2.5580(2) Å is among the shortest observed for dinuclear gold complexes bearing PY ligands.²⁹

3-OTf₂ crystallizes in the space group $P\bar{1}$ with two molecules of $[\mathbf{3}]^{2+}$ and four OTf^- ions in the asymmetric unit (Figure 1b). The complex adopts a boat conformation with the gold(III) centers in square planar coordination environments. Each gold coordination sphere contains the PY ligands in a *trans* arrangement, the $\mu\text{-CH}_2$ ligand, and a coordinated MeCN molecule. The $\text{Au}-\text{C}_{\text{PY}}$ (2.031(17)–2.148(16) Å) and $\text{Au}-\text{C}_{29}$ (1.988(14)–2.060(16) Å) distances are similar to those observed in related structures.^{19,21} The $\text{Au}-\text{Au}$ distances (3.0673(10) and 3.065(18) Å) are within the sum of the van der Waals radii (3.32 Å), but longer than the sum of the covalent radii (2.88 Å). This may suggest the presence of weak aurophilic interactions, but these are rare for gold(III) and most prevalent with face-to-face pairing of square planar complexes.^{30–32}

With **2-OTf**₂ and **3-OTf**₂ in hand, we sought to investigate their activity as Lewis acid catalysts. Cationic gold(I) and gold(III) complexes have demonstrated contrasting reactivity for the Lewis acid catalyzed addition of silyl enol ethers to α,β -unsaturated carbonyl compounds.¹² Thus, we decided to screen **2-OTf**₂ and **3-OTf**₂ as catalysts for the addition of silyl enol ether **4** to crotonaldehyde (**5a**) and cyclohexenone (**5b**) (Table

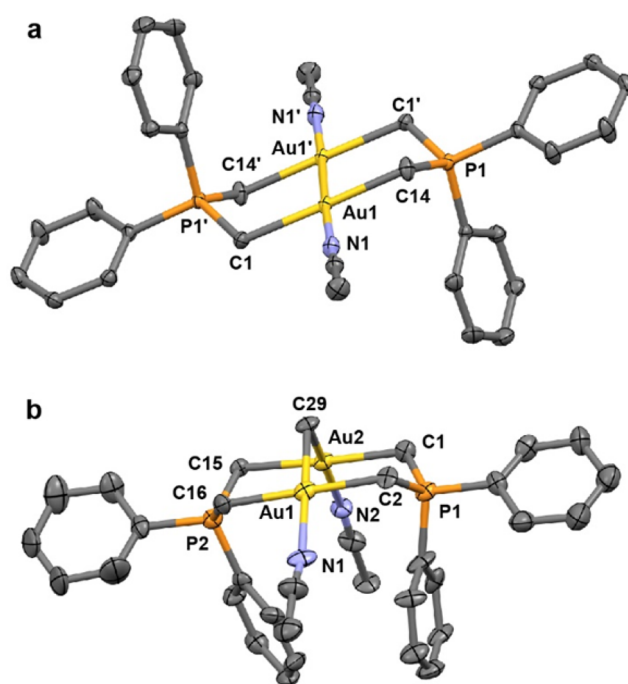


Figure 1. Solid-state structures of **2-OTf**₂ (a) and **3-OTf**₂ (b). All hydrogen atoms, solvent molecules, and OTf^- counterions have been omitted for clarity. Only one of two independent molecules in the asymmetric unit of **3-OTf**₂ is shown. Pertinent metrical parameters can be found in the text and Supporting Information.

1). We also sought to compare the activity of the gold PY complexes with gold(I) Lewis acids. Although the cationic gold(I) PY complex $[\text{Au}(\text{CH}_2\text{PPh}_3)]^+$ would seem suitable for

Table 1. Gold-Catalyzed Mukaiyama Additions^a

entry	catalyst	cat. loading	substrate	% yield ^b	
				6	7
1	2-OTf ₂	4%	5a	68	27
2	3-OTf ₂	4%	5a	70	26
3	$\text{Ph}_3\text{PAuOTf}^c$	4%	5a	62	31
4	IPrAuOTf^c	4%	5a	0	0
5	2-Cl ₂	4%	5a	0	0
6	3-Br ₂	4%	5a	0	0
7	AgOTf	4%	5a	0	0
8	2-OTf ₂	4%	5b	0	88
9	3-OTf ₂	4%	5b	0	45
10	$\text{Ph}_3\text{PAuOTf}^c$	4%	5b	0	20
11	IPrAuOTf^c	4%	5b	0	0
12	2-OTf ₂	2%	5a	67	27
13	2-OTf ₂	0.5%	5a	65	26
14	$\text{Ph}_3\text{PAuOTf}^c$	0.5%	5a	0	0

^aReaction conditions: **5a/b** (0.1 mmol), **4** (0.1 mmol), CH_2Cl_2 (0.5 mL), C_6D_6 (0.1 mL), 25 °C, 12 h. ^bDetermined by ^1H NMR with respect to an internal standard (trimethoxybenzene) at 12 h. ^cGenerated *in situ* from $\text{LAuCl}/\text{AgOTf}$. See Supporting Information for details.

this purpose, it has previously demonstrated poor catalytic activity owing to decomposition.³³ Therefore, the commonly employed Lewis acid catalysts Ph_3PAuOTf and IPrAuOTf were chosen for comparison.¹

The addition reactions were carried out at room temperature in CH_2Cl_2 solution with 4 mol % of catalyst and were monitored by ^1H NMR spectroscopy (Table 1). 2-OTf_2 provided nearly complete conversion of **5a** after 1 h, while the reaction with 3-OTf_2 required over 10 h to reach complete conversion (Figure 2). Analysis of the first-order rate plots

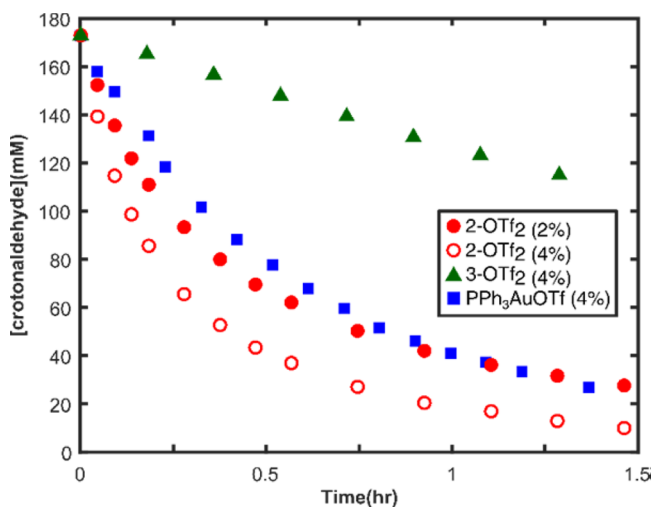


Figure 2. Reaction profile for the addition of **4** to crotonaldehyde (**5a**) in the presence of 2-OTf_2 (circles), 3-OTf_2 (triangles), or Ph_3PAuOTf (squares).

revealed initial observed rate constants (k_{obs}) of 1.1×10^{-3} and $8.4 \times 10^{-5} \text{ s}^{-1}$ with 2-OTf_2 and 3-OTf_2 , respectively (Figures S9 and S10). Furthermore, a mixture of aldol (**6a**) and conjugate addition (**7a**) products was observed in a ca. 2.5:1 ratio for both catalysts (entries 1 and 2).

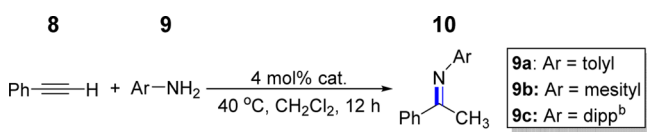
The reaction of **4** and **5a** was carried out under the same conditions using *in situ* generated Ph_3PAuOTf and IPrAuOTf as catalysts (entries 3 and 4). While Ph_3PAuOTf provided nearly complete conversion of **5a** within 1.5 h, no reaction was observed with IPrAuOTf after 12 h. The product selectivity with Ph_3PAuOTf (**6a**:**7a** = 2:1) was similar to that observed for 2-OTf_2 . Complexes **3-Br₂** and **2-Cl₂** showed no catalytic activity for the reaction, confirming that halide exchange for the more weakly coordinating OTf^- anion is necessary to activate the gold centers for catalysis (entries 5 and 6). In addition, AgOTf exhibited no catalytic activity under the reaction conditions (entry 7).

With cyclohexenone (**5b**) as a substrate, only the conjugate addition product (**7b**) was observed. 2-OTf_2 provided 90% conversion of cyclohexenone after 12 h, while the reaction with 3-OTf_2 reached only 50% conversion in 12 h (entries 8 and 9). Analysis of the first-order rate plots revealed initial observed rate constants (k_{obs}) of 1.5×10^{-4} and $1.1 \times 10^{-5} \text{ s}^{-1}$ with 2-OTf_2 and 3-OTf_2 , respectively (Figures S11 and S12). While Ph_3PAuOTf provided 25% conversion after 12 h, no reaction was observed with IPrAuOTf after 12 h (entries 10 and 11). These results follow the same trend observed with crotonaldehyde, but the overall reaction rates are slowed by roughly a factor of 10 (Figure S13).

Since the adjacent gold centers in 2-OTf may both participate in substrate activation and catalysis, we evaluated its catalytic efficiency at 2 mol % (4 mol % Au) loading (entry 12). Analysis of the reaction profile revealed that 2 mol % 2-OTf provides a similar rate to 4 mol % Ph_3PAuOTf for the addition reaction with crotonaldehyde (Figure 2). This suggests that Ph_3PAuOTf and 2-OTf have similar catalytic efficiencies on a per gold basis. However, when the catalyst loadings were lowered to 0.5 mol %, 2-OTf provided complete conversion of crotonaldehyde after 12 h, while no reaction was observed with Ph_3PAuOTf (entries 13 and 14). This indicates that 2-OTf is less prone to deactivation by trace impurities than Ph_3PAuOTf .³⁴

Recently, the Gutmann–Beckett method has been used to gauge the relative Lewis acidity of gold complexes.^{12,35,36} We decided to employ this method in order to gain insight into the origin of the different catalytic activities of the gold complexes in this study. Solutions of 2-OTf_2 and 3-OTf_2 in CH_2Cl_2 were treated with two equivalents of Et_3PO , and the difference in ^{31}P NMR chemical shift ($\Delta\delta$) between an Et_3PO internal standard ($\delta = 50$) and gold-coordinated Et_3PO species was calculated as a measure of relative Lewis acid strengths. The ^{31}P NMR spectrum of $3\text{-OTf}_2/\text{Et}_3\text{PO}$ shows three distinct ylide resonances that correspond to an equilibrium mixture of the parent complex and the 1:1 and 2:1 Et_3PO adducts (Figure S36). A sharp resonance at 73 ppm ($\Delta\delta = 25$) was assigned to coordinated Et_3PO in the 2:1 adduct. The room-temperature ^{31}P NMR spectrum of $2\text{-OTf}_2/\text{Et}_3\text{PO}$ exhibits a sharp ylide resonance at 32 ppm and a very broad signal around 53 ppm that suggests the rate of Et_3PO exchange is close to the time scale of the NMR experiment (Figure S37). The broad signal decoalesced upon cooling the sample to -45°C , and resonances corresponding to coordinated Et_3PO appeared at 75 and 76 ppm ($\Delta\delta = 25\text{--}26$). Additional ylide resonances also began to emerge around 32 ppm, but were too poorly resolved to determine the speciation at this temperature. When a solution of IPrAuOTf in CH_2Cl_2 was treated with one equivalent of Et_3PO , a sharp ^{31}P NMR signal corresponding to the adduct appeared at 80 ppm ($\Delta\delta = 30$) (Figure S38). At room temperature, an equimolar mixture of Ph_3PAuOTf and Et_3PO gives rise to a single PPh_3 resonance at 26 ppm and a broad signal around 71 ppm (Figure S39). The broad signal did not fully decoalesce upon cooling to -45°C . The $\Delta\delta$ values determined from this study suggest that 2-OTf_2 and 3-OTf_2 exhibit comparable Lewis acidities ($\Delta\delta = 25\text{--}26$) and IPrAuOTf is a slightly stronger Lewis acid ($\Delta\delta = 30$). No meaningful comparison can be made with Ph_3PAuOTf since peak decoalescence was not observed. Interestingly, the ligand exchange equilibria and dynamics of these complexes are very different. At room temperature, Et_3PO ligand exchange occurs more rapidly for 2-OTf_2 and Ph_3PAuOTf than for 3-OTf_2 and IPrAuOTf . While catalytic efficiency for the enone additions seems to better correlate with ligand exchange rates than apparent Lewis acidity, further studies will be necessary to fully elucidate the steric and electronic factors that influence catalytic activity.

Next, we decided to probe the ability of 2-OTf_2 and 3-OTf_2 to activate C–C π bonds by screening their activity for the hydroamination of phenylacetylene (**8**) with aryl amines **9a–c**. These reactions were carried out in the presence of 4 mol % of each catalyst and monitored by ^1H NMR spectroscopy (Table 2). 3-OTf_2 and IPrAuOTf proved to be the most efficient catalysts when toluidine (**9a**) was used as the nucleophile

Table 2. Gold-Catalyzed Hydroamination^a


entry	catalyst	ArNH ₂	% conv ^c	% yield ^d
1	2-OTf ₂	9a	57	54
2	2-OTf ₂	9b	83	77
3	2-OTf ₂	9c	83	81
4	3-OTf ₂	9a	76	63
5	3-OTf ₂	9b	38	34
6	3-OTf ₂	9c	35	32
7	Ph ₃ PAuOTf ^e	9a	38	25
8	Ph ₃ PAuOTf ^e	9b	63	54
9	Ph ₃ PAuOTf ^e	9c	67	64
10	IPrAuOTf ^e	9a	72	69
11	IPrAuOTf ^e	9b	40	39
12	IPrAuOTf ^e	9c	83	79

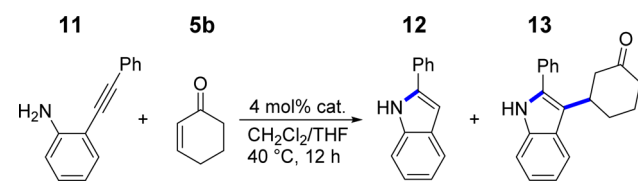
^aReaction conditions: phenylacetylene (0.1 mmol), aryl amine (0.1 mmol), catalyst (0.004 mmol), CH₂Cl₂ (0.5 mL), C₆D₆ (0.1 mL), 40 °C, 12 h. ^bdipp = 2,6-diisopropylphenyl. ^cBased on consumption of aryl amine at 12 h. ^dDetermined by ¹H NMR with respect to an internal standard (1,3,5-trimethoxybenzene) at 12 h. ^eGenerated *in situ* from LAuCl/AgOTf. See Supporting Information for details.

(entries 4 and 10). The catalytic activity of 3-OTf₂ decreased with the more sterically hindered amines 9b and 9c (entries 5 and 6), while 2-OTf₂ and Ph₃PAuOTf exhibited improved activity with the larger aryl amine substrates. IPrAuOTf showed decreased conversion with substrate 9b, but good activity for the larger aniline 9c. This peculiar trend was reproducible over several runs and with different batches of catalyst and substrate.

Amine coordination to Lewis acid catalyst sites is competitive with alkyne activation in hydroamination reactions.^{37–42} The rigid boat conformation of the metallacycle in 3-OTf₂ results in increased steric crowding around the gold coordination sites compared to 2-OTf₂. This steric crowding may suppress strong binding of the relatively unhindered amine 9a to the gold centers in 3-OTf₂, resulting in higher catalytic activity. In the reactions employing sterically bulky 9b and 9c, amine coordination should be less competitive with alkyne activation for all catalysts. Indeed, this would explain the increased catalytic activity of 2-OTf₂ and Ph₃PAuOTf with these substrates. However, 3-OTf₂ exhibits the opposite trend, suggesting that increased steric hindrance may block nucleophile access to the activated alkyne.

From the results above, 2-OTf₂ and 3-OTf₂ exhibit greater versatility as catalysts for Mukaiyama additions and hydroamination of alkynes than Ph₃PAuOTf and IPrAuOTf. We considered that this versatility might be leveraged for use in cascade reactions. In order to test this hypothesis, we screened the activity of the gold catalysts for the cascade reaction of ortho-substituted aniline 11 and cyclohexenone (5b). The reaction involves intramolecular hydroamination to afford 2-phenylindole (12) and subsequent intermolecular conjugate addition to cyclohexenone to generate 2,3-substituted indole 13 (Table 3).^{43–45}

The reaction was carried out at 40 °C in a 1:1 mixture of THF and CH₂Cl₂ solution with 4 mol % of catalyst, and the product distributions were determined by ¹H NMR spectroscopy and GC-MS. While the reaction with 2-OTf₂ delivered indole 13 in good yield, the reactions with 3-OTf₂ and

Table 3. Gold-Catalyzed Cascade Reaction^a


entry	catalyst	% yield 12 ^b	% yield 13 ^b
1	none	0	0
2	HOTf	4	4
3	2-OTf ₂	25	75 (68) ^c
4	3-OTf ₂	78	14
5	Ph ₃ PAuOTf ^d	37	8
6	IPrAuOTf ^d	95 (90) ^c	2

^aReaction conditions: cyclohexenone (0.1 mmol), aniline (0.1 mmol), catalyst (0.004 mmol), CH₂Cl₂ (1.0 mL), THF (1.0 mL), 40 °C, 12 h. ^bDetermined by GC-MS with respect to an internal standard (trimethoxybenzene) at 12 h. ^cIsolated yield in parentheses. ^dGenerated *in situ* from LAuCl/AgOTf. See Supporting Information for details.

Ph₃PAuOTf as catalysts afforded low yields of the cascade product (entries 3–5). Only a trace amount of 13 was observed in the reaction with IPrAuOTf after 12 h, but indole 12 was generated in near-quantitative yield (entry 6). These results are in agreement with previous experiments. While 2-OTf₂ and 3-OTf₂ showed comparable activity as hydroamination catalysts, 2-OTf₂ is a better catalyst for enone additions. This trend is reflected in the higher yield of 13 delivered by 2-OTf₂. Moreover, while IPrAuOTf proves to be a good hydroamination catalyst, it is not competent for the conjugate addition reaction necessary to furnish indole 13. Notably, conducting the reaction in the presence of HOTf did not afford either indole 12 or 13 in good yield, suggesting that adventitious acid formed during the reaction is not responsible for the observed catalysis (entry 2).

CONCLUSIONS

In summary, we report the synthesis, characterization, and catalytic activity of cationic dinuclear gold(II,II) and gold-(III,III) complexes supported by phosphorus ylide ligands. To the best of our knowledge, this is the first reported example of Lewis acid catalysis at gold(II) centers. 2-OTf₂ and 3-OTf₂ catalyze both Mukaiyama addition and alkyne hydroamination reactions, offering similar or improved catalytic activity compared to the gold(I) complexes Ph₃PAuOTf and IPrAuOTf. The ability of 2-OTf₂ and 3-OTf₂ to activate alkynes and enones suggests both soft carbophilic and hard oxophilic Lewis acid character. This hybrid Lewis acidity was further demonstrated in a cascade reaction sequence involving intramolecular hydroamination followed by intermolecular enone addition to generate a 2,3-substituted indole. 2-OTf₂ proved to be a good catalyst for this cascade sequence, while 3-OTf₂ and the commonly used gold(I) catalysts Ph₃PAuOTf and IPrAuOTf were ineffective. Ongoing work is focused on further elucidating the steric and electronic factors that influence the catalytic activity of Lewis acidic gold complexes as well as exploring the utility of dinuclear gold PY complexes in other types of catalysis.

EXPERIMENTAL SECTION

General Considerations. All manipulations were carried out using a nitrogen-filled glovebox or standard Schlenk techniques unless otherwise noted. All glassware was oven-dried in a 150 °C oven before use. Solvents were degassed by sparging with ultra-high-purity argon and dried via passage through columns of drying agents using a solvent purification system from Pure Process Technologies. $\text{Au}_2[\text{PPh}_2(\text{CH}_2)_2]$ (**1**), $\text{Au}_2\text{Br}_2[\text{PPh}_2(\text{CH}_2)_2](\mu\text{-CH}_2)$ (**3-Br**), PPh_3AuCl , IPrAuCl , and 1-phenyl-1-trimethylsilyloxyethylene (**4**) were prepared according to literature procedures.^{18,19,21,46–48} Toluidine and mesitylamine were purified by sublimation and vacuum distillation, respectively. All other chemicals were purchased from commercial vendors and used without further purification. NMR spectra were recorded at ambient temperature on a Varian Inova 400 MHz instrument. ^1H and ^{13}C NMR chemical shifts were referenced to the residual solvent chemical shifts. ^{31}P NMR chemical shifts were referenced to 85% H_3PO_4 , and ^{19}F NMR chemical shifts were referenced to 99% $\text{F}_3\text{CCO}_2\text{H}$. Solvent-suppressed ^1H NMR spectra were collected using the WET1D sequence with default parameters.⁴⁹ Briefly, spectra were collected using selective pulses of 86 ms with the SEDUCE pulse shape. Gradient pulses were 2 ms in duration, had amplitude ratios of 8:4:2:1, and were each followed by an additional 2 ms delay prior to the next RF pulse. The recycle delay between scans was 30 s, 16K points were collected, and the acquisition time was 2.5 s. GC-MS analysis was performed using an Agilent 7890A GC equipped with a HP-5 capillary column (30 m, 0.25 mm i.d., 0.25 μm film thickness) and a 5975C mass spectrometer as detector. The carrier gas was helium, at a flow rate of 1 mL/min. For MS detection an electron ionization system was used with an ionization energy of 70 eV.

Synthesis of $[\text{AuPY}]_2\text{Cl}_2$ (2-Cl**).** This compound was prepared using a modified literature procedure.⁵⁰ A solution of PhICl_2 (17 mg, 0.062 mmol) in CH_2Cl_2 (1.0 mL) was added dropwise to a stirring solution of $\text{Au}_2[\text{PPh}_2(\text{CH}_2)_2]$ (**1**) (51 mg, 0.062 mmol) in CH_2Cl_2 (1.0 mL). The reaction mixture initially turned bright green, but the color faded to a pale yellow by the end of the addition. The reaction was stirred for an additional 15 min. The reaction mixture was concentrated to half of the original volume, and diethyl ether (5 mL) was added, resulting in formation of a bright yellow precipitate. The precipitate was collected by centrifugation and washed with additional diethyl ether (3 \times 5 mL). The precipitate was dried *in vacuo* to afford a crystalline, bright yellow powder. Yield: 50 mg, 90% yield. The ^1H and ^{31}P NMR spectral data matched those reported in the literature.^{18,51}

Synthesis of $[\text{Au}_2(\mu\text{-PY})_2(\text{MeCN})_2]\text{OTf}_2$ (2-OTf**).** The following reaction was carried out in a 20 mL scintillation vial wrapped in black electrical tape to rigorously exclude light. A solution of **2-Cl** (20 mg, 0.022 mmol) in CH_2Cl_2 (1.0 mL) was added dropwise to a stirring suspension of AgOTf (12 mg, 0.047 mmol) in MeCN (1.0 mL). The reaction was stirred for an additional 30 min and then concentrated *in vacuo*. The resulting residue was extracted with CH_2Cl_2 (5 mL), and the mixture was filtered through a 0.45 μm PTFE syringe filter to give a clear, orange solution. Acetonitrile (0.1 mL) was added to the filtrate, furnishing a yellow solution, and the reaction was concentrated *in vacuo*, resulting in precipitation of the product as a bright yellow crystalline solid. X-ray quality crystals were obtained by vapor diffusion of diethyl ether into a concentrated solution of **2-OTf** in acetonitrile. Yield: 21 mg, 84%. ^1H NMR (400 MHz, CD_2Cl_2): δ 7.61–7.53 (m, 12H, Ar-H), 7.50–7.46 (m, 8H, Ar-H), 2.20 (s, 6H, MeCN), 1.96 (d, 8H, $^2J_{\text{PH}} = 10.2$ Hz, PY- CH_2). $^{31}\text{P}\{^1\text{H}\}$ NMR (161.8 MHz, CD_2Cl_2): δ 34.5 (s). ^{19}F NMR (376.4 MHz, CD_2Cl_2): δ -77.3 (s). $^{13}\text{C}\{^1\text{H}\}$ NMR (100.5 MHz, CD_2Cl_2): δ 133.32 (s), 131.2 (d, $^2J_{\text{PC}} = 9.1$ Hz), 131.1 (s), 129.9 (d, $^2J_{\text{PC}} = 11.4$ Hz), 129.9 (s), 14.6 (d, $^1J_{\text{PC}} = 60.3$ Hz), 2.8 (s). Anal. Calcd for $\text{C}_{30}\text{H}_{28}\text{Au}_2\text{F}_6\text{O}_6\text{P}_2\text{S}_2 + 1.5 \text{C}_2\text{H}_3\text{N}$: C, 33.58; H, 2.78; N, 1.78. Found: C, 33.33; H, 2.82; N, 1.81 (approximately 0.5 equiv. of acetonitrile was lost in drying).

Synthesis of $[\text{Au}_2(\mu\text{-PY})_2(\mu\text{-CH}_2)(\text{MeCN})_2]\text{OTf}_2$ (3-OTf**).** A solution of **3-Br** (30 mg, 0.03 mmol) in CH_2Cl_2 (1.0 mL) was added dropwise to a stirring suspension of AgOTf (16.0 mg, 0.062 mmol) in CH_2Cl_2 (1.0 mL). Following completion of the addition, the reaction was stirred for an additional 30 min. The reaction was filtered

through a 0.45 μm PTFE syringe filter and then concentrated *in vacuo* to afford the product as an off-white powder. X-ray quality crystals were obtained by vapor diffusion of diethyl ether into a concentrated solution of **3-OTf** in acetonitrile. Yield: 31 mg, 94%. ^1H NMR (400 MHz, CD_3CN): δ 7.64–7.48 (m, 16H, Ar-H), 7.46 (t, 4H, $^3J_{\text{PH}} = 7.4$ Hz, Ar-H), 2.68 (s, 2H, $\mu\text{-CH}_2$), 2.46 (dd, 4H, $^2J_{\text{PH}} = 12.9$ Hz, $^3J_{\text{HH}} = 12.9$ Hz, PY- CH_2), 1.97 (s, 6H, MeCN), 1.88 (dd, 4H, $^2J_{\text{PH}} = 12.1$ Hz, $^2J_{\text{HH}} = 12.1$ Hz, PY- CH_2). $^{31}\text{P}\{^1\text{H}\}$ NMR (161.8 MHz, CD_3CN): δ 35.1 (s). ^{19}F NMR (376.4 MHz, CD_3CN): δ -77.8 (s). $^{13}\text{C}\{^1\text{H}\}$ NMR (100.5 MHz, CD_3CN): δ 138.8 (s), 137.9 (s), 137.7 (d, $^1J_{\text{PC}} = 70.2$ Hz), 135.8 (t, $^2J_{\text{PC}} = 4.5$ Hz), 135.4 (t, $^2J_{\text{PC}} = 4.5$ Hz), 134.7 (m), 129.4 (d, $^1J_{\text{PC}} = 90.8$ Hz), 19.5 (d, $^1J_{\text{PC}} = 48.8$ Hz), 18.4 (s). Anal. Calcd for $\text{C}_{31}\text{H}_{30}\text{Au}_2\text{F}_6\text{O}_6\text{P}_2\text{S}_2 + 1.33 \text{C}_2\text{H}_3\text{N}$: C, 34.05; H, 2.89; N, 1.57. Found: C, 33.75; H, 3.17; N, 1.58 (approximately 0.66 equiv of acetonitrile was lost in drying).

Generation of PPh_3AuOTf and IPrAuOTf . Catalyst stock solutions (13.3 mM) of PPh_3AuOTf and IPrAuOTf were prepared by addition of AgOTf (0.040 mmol) to CH_2Cl_2 solutions (3.0 mL) of PPh_3AuCl and IPrAuCl (0.040 mmol), respectively. The mixtures were allowed to stir for 30 min, and the precipitated AgCl was removed by filtration using a 0.45 μm PTFE syringe filter.^{34,52–54} The resulting catalyst solutions were used immediately.

General Procedure for Mukaiyama Addition Reactions. In a N_2 -filled glovebox, a vial was charged with **4** (0.1 mmol), **5a/b** (0.1 mmol), CH_2Cl_2 (0.2 mL), and C_6D_6 (0.1 mL). The appropriate amount of catalyst or catalyst stock solution was added (see Table 1), and CH_2Cl_2 was added to reach a total reaction volume of 0.6 mL. For runs that involved monitoring reaction progress, hexamethylbenzene (0.01–0.05 mmol) was added as an internal standard and the reaction mixtures were transferred to NMR tubes. For all other runs, the reactions were quenched after 12 h with 10:1 MeOH/1 M HCl (0.1 mL), filtered over a plug of silica, and concentrated to dryness. The crude residues were then extracted with CDCl_3 , and a known amount of trimethoxybenzene (0.01–0.05 mmol) was added as an internal standard. The product yields were determined by integration of the ^1H NMR spectra.

General Procedure for Hydroamination Reactions. In a N_2 -filled glovebox, a vial was charged with **8** (0.1 mmol), **9a/b/c** (0.1 mmol), CH_2Cl_2 (0.2 mL), and C_6D_6 (0.1 mL). The appropriate amount of catalyst or catalyst stock solution was added (see Table 2), and CH_2Cl_2 was added to reach a total reaction volume of 0.6 mL. A known amount of trimethoxybenzene (0.01–0.05 mmol) was then added as an internal standard. The reaction mixtures were transferred to an NMR tube and heated at 40 °C for 12 h. The yields were determined by ^1H NMR spectroscopy.

General Procedure for Cascade Reaction of **11 and **5b**.** In a N_2 -filled glovebox, a vial was charged with **11** (0.1 mmol), **5b** (0.1 mmol), catalyst (0.004 mmol), CH_2Cl_2 (1.0 mL), and THF (1.0 mL). The reaction mixture was heated at 40 °C for 12 h in a sealed vial. The reaction was filtered over a plug of silica and concentrated to dryness. The residue was extracted with CDCl_3 , and a known amount of trimethoxybenzene (0.01–0.05 mmol) was added as an internal standard. The product yield was determined by ^1H NMR spectroscopy and GC-MS.

ASSOCIATED CONTENT

Supporting Information

The Supporting Information is available free of charge on the ACS Publications website at DOI: 10.1021/acs.organomet.6b00403.

Additional experimental procedures and NMR and GC-MS characterization data (PDF)

Crystallographic data for **2-OTf** and **3-OTf** (CIF)

AUTHOR INFORMATION

Corresponding Author

*E-mail: cwade@brandeis.edu.

Notes

The authors declare no competing financial interest.

ACKNOWLEDGMENTS

C.R.W. acknowledges Brandeis University for start-up funding.

REFERENCES

- (1) Gorin, D. J.; Sherry, B. D.; Toste, F. D. *Chem. Rev.* **2008**, *108*, 3351.
- (2) Rosca, D. A.; Wright, J. A.; Bochmann, M. *Dalton Trans.* **2015**, *44*, 20785.
- (3) Joost, M.; Amgoune, A.; Bourissou, D. *Angew. Chem., Int. Ed.* **2015**, *54*, 15022.
- (4) Hashmi, A. S.; Hutchings, G. J. *Angew. Chem., Int. Ed.* **2006**, *45*, 7896.
- (5) Pflasterer, D.; Hashmi, A. S. *Chem. Soc. Rev.* **2016**, *45*, 1331.
- (6) Dorel, R.; Echavarren, A. M. *Chem. Rev.* **2015**, *115*, 9028.
- (7) de Frémont, P.; Singh, R.; Stevens, E. D.; Petersen, J. L.; Nolan, S. P. *Organometallics* **2007**, *26*, 1376.
- (8) Shen, H. C. *Tetrahedron* **2008**, *64*, 3885.
- (9) Sromek, A. W.; Rubina, M.; Gevorgyan, V. *J. Am. Chem. Soc.* **2005**, *127*, 10500.
- (10) Morita, N.; Yasuda, A.; Shibata, M.; Ban, S.; Hashimoto, Y.; Okamoto, I.; Tamura, O. *Org. Lett.* **2015**, *17*, 2668.
- (11) Reetz, M. T.; Sommer, K. *Eur. J. Org. Chem.* **2003**, *2003*, 3485.
- (12) Wu, C. Y.; Horibe, T.; Jacobsen, C. B.; Toste, F. D. *Nature* **2015**, *517*, 449.
- (13) Tkatchouk, E.; Mankad, N. P.; Benitez, D.; Goddard, W. A., 3rd; Toste, F. D. *J. Am. Chem. Soc.* **2011**, *133*, 14293.
- (14) Laguna, A.; Laguna, M. *Coord. Chem. Rev.* **1999**, *193–195*, 837.
- (15) Mirzadeh, N.; Bennett, M. A.; Bhargava, S. K. *Coord. Chem. Rev.* **2013**, *257*, 2250.
- (16) Transient gold(II) species have been implicated as intermediates in catalysis with dinuclear gold(I,I) complexes: Revol, G.; McCallum, T.; Morin, M.; Gagosz, F.; Barriault, L. *Angew. Chem., Int. Ed.* **2013**, *52*, 13342. Levin, M. D.; Toste, F. D. *Angew. Chem., Int. Ed.* **2014**, *53*, 6211. Xie, J.; Zhang, T.; Chen, F.; Mehrkens, N.; Rominger, F.; Rudolph, M.; Hashmi, A. S. *Angew. Chem., Int. Ed.* **2016**, *55*, 2934.
- (17) Fackler, J. P. *Polyhedron* **1997**, *16*, 1.
- (18) Basil, J. D.; Murray, H. H.; Fackler, J. P.; Tocher, J.; Mazany, A. M.; Trzcinska-Bancroft, B.; Knachel, H.; Dudis, D.; Delord, T. J.; Marler, D. *J. Am. Chem. Soc.* **1985**, *107*, 6908.
- (19) Schmidbaur, H.; Hartmann, C.; Riede, J.; Huber, B.; Mueller, G. *Organometallics* **1986**, *5*, 1652.
- (20) Schmidbaur, H.; Jandik, P. *Inorg. Chim. Acta* **1983**, *74*, 97.
- (21) Jandik, P.; Schubert, U.; Schmidbaur, H. *Angew. Chem., Int. Ed. Engl.* **1982**, *21*, 73.
- (22) Schmidbaur, H.; Franke, R. *Angew. Chem., Int. Ed. Engl.* **1973**, *12*, 416.
- (23) Wolf, W. J.; Winston, M. S.; Toste, F. D. *Nat. Chem.* **2014**, *6*, 159.
- (24) Kawai, H.; Wolf, W. J.; DiPasquale, A. G.; Winston, M. S.; Toste, F. D. *J. Am. Chem. Soc.* **2016**, *138*, 587.
- (25) Hashmi, A. S. K.; Blanco, M. C.; Fischer, D.; Bats, J. W. *Eur. J. Org. Chem.* **2006**, *2006*, 1387.
- (26) Bardají, M.; Gimeno, M. C.; Jiménez, J.; Laguna, A.; Laguna, M.; Jones, P. G. *J. Organomet. Chem.* **1992**, *441*, 339.
- (27) Laguna, A.; Laguna, M.; Jimenez, J.; Lahoz, F. J.; Olmos, E. *Organometallics* **1994**, *13*, 253.
- (28) Trzcinska-Bancroft, B.; Khan, M. N. I.; Fackler, J. P. *Organometallics* **1988**, *7*, 993.
- (29) Porter, L. C.; Fackler, J. P., Jr. *Acta Crystallogr., Sect. C: Cryst. Struct. Commun.* **1986**, *42*, 1128.
- (30) Hayoun, R.; Zhong, D. K.; Rheingold, A. L.; Doerrner, L. H. *Inorg. Chem.* **2006**, *45*, 6120.
- (31) Doerrner, L. H. *Dalton Trans.* **2010**, *39*, 3543.
- (32) Klapotke, T. M.; Krumm, B.; Galvez-Ruiz, J. C.; Noth, H. *Inorg. Chem.* **2005**, *44*, 9625.
- (33) Cordon, J.; López-de-Luzuriaga, J. M.; Monge, M. *Organometallics* **2016**, *35*, 732.
- (34) Kumar, M.; Hammond, G. B.; Xu, B. *Org. Lett.* **2014**, *16*, 3452.
- (35) Yang, H.; Gabbai, F. P. *J. Am. Chem. Soc.* **2015**, *137*, 13425.
- (36) Tlahuext-Aca, A.; Hopkinson, M. N.; Daniliuc, C.; Glorius, F. *Chem. - Eur. J.* **2016**, DOI: 10.1002/chem.201602649.
- (37) Lavallo, V.; Wright, J. H., 2nd; Tham, F. S.; Quinlivan, S. *Angew. Chem., Int. Ed.* **2013**, *52*, 3172.
- (38) Katari, M.; Rao, M. N.; Rajaraman, G.; Ghosh, P. *Inorg. Chem.* **2012**, *51*, 5593.
- (39) Zhdanko, A.; Maier, M. E. *Angew. Chem., Int. Ed.* **2014**, *53*, 7760.
- (40) Zeng, X.; Soleilhavoup, M.; Bertrand, G. *Org. Lett.* **2009**, *11*, 3166.
- (41) Lavallo, V.; Frey, G. D.; Donnadieu, B.; Soleilhavoup, M.; Bertrand, G. *Angew. Chem., Int. Ed.* **2008**, *47*, 5224.
- (42) Khin, C.; Hashmi, A. S. K.; Rominger, F. *Eur. J. Inorg. Chem.* **2010**, *2010*, 1063.
- (43) Hashmi, A. S. K.; Ramamurthi, T. D.; Rominger, F. *Adv. Synth. Catal.* **2010**, *352*, 971.
- (44) Hashmi, A. S. K.; Schwarz, L.; Choi, J.-H.; Frost, T. M. *Angew. Chem., Int. Ed.* **2000**, *39*, 2285.
- (45) Dyker, G.; Muth, E.; Hashmi, A. S. K.; Ding, L. *Adv. Synth. Catal.* **2003**, *345*, 1247.
- (46) Lin, J.; Liu, B. *Synth. Commun.* **1997**, *27*, 739.
- (47) Collado, A.; Gomez-Suarez, A.; Martin, A. R.; Slawin, A. M.; Nolan, S. P. *Chem. Commun.* **2013**, *49*, 5541.
- (48) Müller, T. E.; Green, J. C.; Mingos, D. M. P.; McPartlin, C. M.; Whittingham, C.; Williams, D. J.; Woodroffe, T. M. *J. Organomet. Chem.* **1998**, *551*, 313.
- (49) Smallcombe, S. H.; Patt, S. L.; Keifer, P. A. *J. Magn. Reson., Ser. A* **1995**, *117*, 295.
- (50) Mendez, L. A.; Jimenez, J.; Cerrada, E.; Mohr, F.; Laguna, M. *J. Am. Chem. Soc.* **2005**, *127*, 852.
- (51) Fackler, J. P.; Trzcinska-Bancroft, B. *Organometallics* **1985**, *4*, 1891.
- (52) Lu, Z.; Han, J.; Hammond, G. B.; Xu, B. *Org. Lett.* **2015**, *17*, 4534.
- (53) Homs, A.; Escofet, I.; Echavarren, A. M. *Org. Lett.* **2013**, *15*, 5782.
- (54) Wang, D.; Cai, R.; Sharma, S.; Jirak, J.; Thummanapelli, S. K.; Akhmedov, N. G.; Zhang, H.; Liu, X.; Petersen, J. L.; Shi, X. *J. Am. Chem. Soc.* **2012**, *134*, 9012.